Flux tubes and confinement

M. Baker, V. Chelnokov, L. Cosmai, F. Cuteri, A. Papa
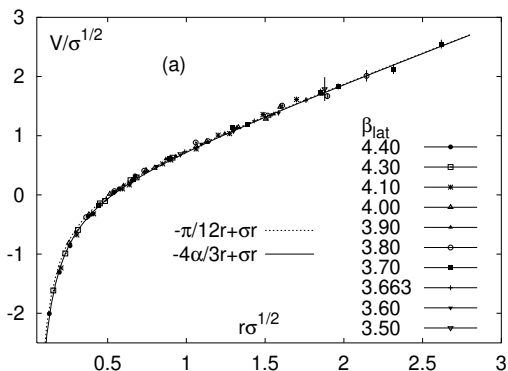
Outline

Confining potential

Heavy quark potential – free energy of a static quark-antiquark configuration separated by a distance d.

$$\langle W(d,t) \rangle = \exp(-tV(d,t)) \ , \quad \lim_{t \to \infty} V(d,t) = -\frac{\pi}{12}\frac{1}{d} + \sigma d$$

Figure (a): $V/\sigma^{1/2}$ versus $r\sigma^{1/2}$, with curves $-\pi/12r + \sigma r$ (dotted) and $-4\alpha/3r + \sigma r$ (solid), for β_{lat} values 4.40, 4.30, 4.10, 4.00, 3.90, 3.80, 3.70, 3.663, 3.60, 3.50.

⬥ Kaczmarek, Zantow (2005)

# Field energy

Energy density can be found from

$$\epsilon(x) = \frac{1}{2}(\vec{\boldsymbol{E}}(x)^2 + \vec{\boldsymbol{B}}(x)^2)$$

○ The chromoelectric field between a static quark and an antiquark forms tube-like structures connecting them. This creates a linear confining potential.

○ The field distributions can be extracted from the lattice simulations, and used to visualize the flux tube, and study its structure.
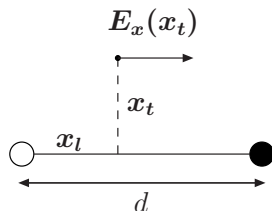
Field energy

Energy density can be found from

$$\epsilon(x) = \frac{1}{2}(\vec{\boldsymbol{E}}(x)^2 + \vec{\boldsymbol{B}}(x)^2)$$


Bali, Schilling, Schlichter (1994)
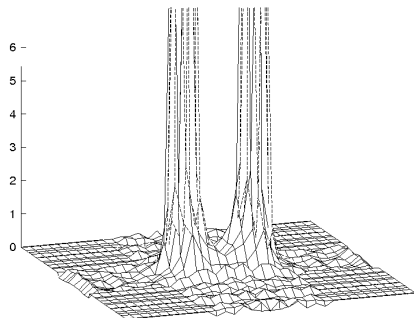
Two interpretations of a flux tube

▶ Abrikosov vortex in a dual superconductor:
  narrow exponentially decaying profile, characterised by London
  penetration length λ;

▶ fluctuating quantum Nambu-Goto string:
  Gaussian profile, logarithmic widening with distance.

The system has cylindrical symmetry, so we can limit ourselves to studying just the (x_l, x_t) plane.
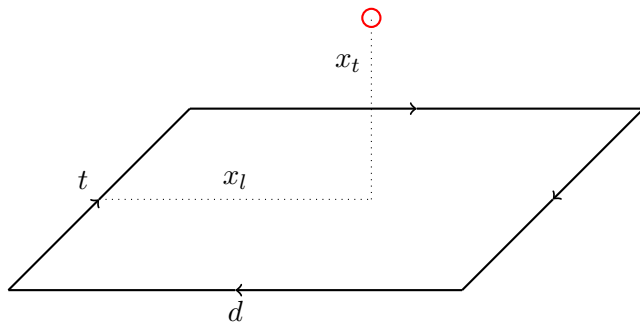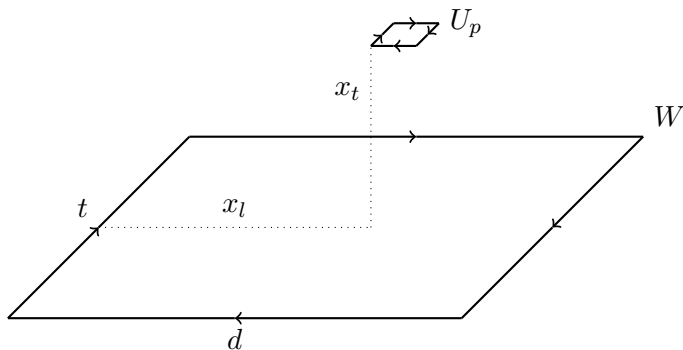
The system has cylindrical symmetry, so we can limit ourselves to studying just the (x_l, x_t) plane.

Measuring the flux tube

Disconnected correlator

$$\left\langle \pm \boldsymbol{F}_{\mu\nu}^2 \right\rangle = \frac{\beta}{a^4} \left[\frac{\langle \operatorname{Tr} W \operatorname{Tr} U_p \rangle}{\langle \operatorname{Tr} W \rangle} - \langle \operatorname{Tr} U_p \rangle \right]$$

Measuring the flux tube

Disconnected correlator

$$\left\langle \pm \boldsymbol{F}_{\mu\nu}^2 \right\rangle = \frac{\beta}{a^4} \left[\frac{\left\langle \operatorname{Tr} W \operatorname{Tr} U_p \right\rangle}{\left\langle \operatorname{Tr} W \right\rangle} - \left\langle \operatorname{Tr} U_p \right\rangle \right]$$

▶ Samples squares of the fields
▶ Includes all SU(3) components and fluctuations
▶ Hard to determine the part that corresponds to linear behavior

Measuring the flux tube

Disconnected correlator

$$\left\langle \pm \boldsymbol{F}_{\mu\nu}^2 \right\rangle = \frac{\beta}{a^4} \left[\frac{\left\langle \operatorname{Tr} W \operatorname{Tr} U_p \right\rangle}{\left\langle \operatorname{Tr} W \right\rangle} - \left\langle \operatorname{Tr} U_p \right\rangle \right]$$

🔗 Bicudo, Cardoso, Cardoso (2017)

Measuring the flux tube
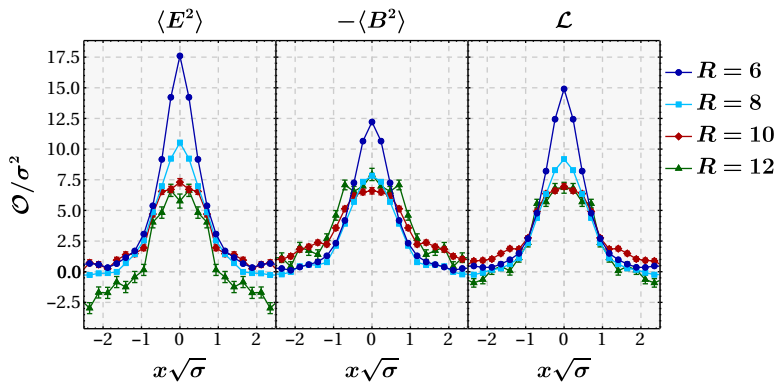
Stress-energy tensor

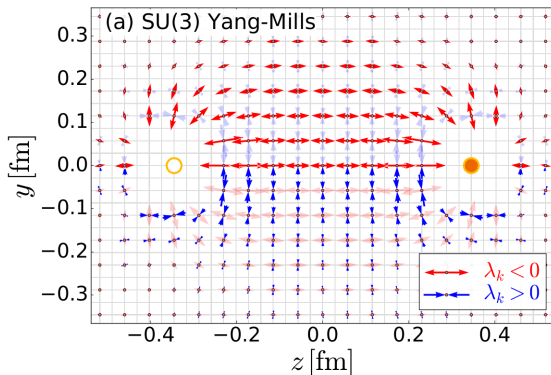$$\mathcal{T}_{\mu\nu}(x) = \frac{1}{g_0^2}\left(F_{\mu\alpha}^a(x)F_{\alpha\nu}^a(x) - g_{\mu\nu}\frac{1}{4}F_{\alpha\beta}^a(x)F_{\alpha\beta}^a(x)\right) \ , \quad \epsilon(x) = -\mathcal{T}_{44}(x)$$

▶ Directly sample energy density
▶ Includes all SU(3) components and fluctuations
▶ Special renormalization procedure ⊘ Suzuki (2015)
▶ Hard to determine the part that corresponds to linear behavior

Measuring the flux tube

Stress-energy tensor

$$\mathcal{T}_{\mu\nu}(x) = \frac{1}{g_0^2} \left(F_{\mu\alpha}^a(x) F_{\alpha\nu}^a(x) - g_{\mu\nu} \frac{1}{4} F_{\alpha\beta}^a(x) F_{\alpha\beta}^a(x) \right) \ , \quad \epsilon(x) = -\mathcal{T}_{44}(x)$$
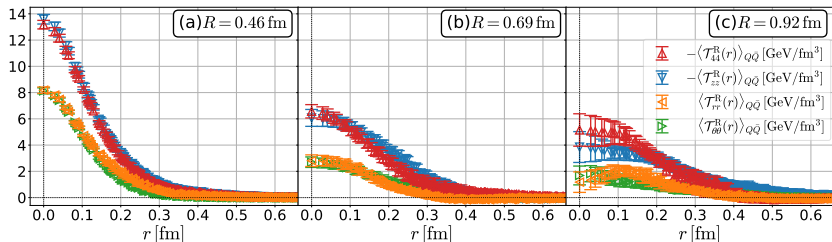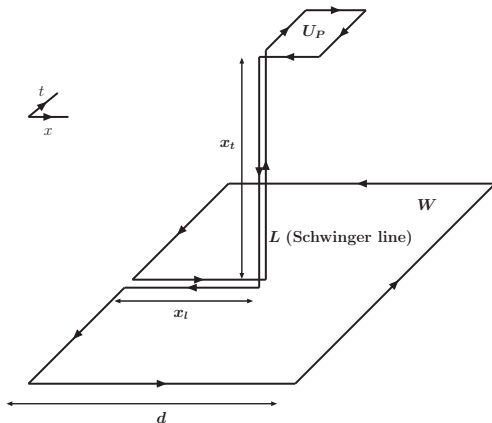

(a) SU(3) Yang-Mills

$\lambda_k < 0$
$\lambda_k > 0$

🔗 Yanagihara, Iritani, Kitazawa, Asakawa, Hatsuda (2019)

Measuring the flux tube

Stress-energy tensor

$$\mathcal{T}_{\mu\nu}(x) = \frac{1}{g_0^2}\left(F^a_{\mu\alpha}(x)F^a_{\alpha\nu}(x) - g_{\mu\nu}\frac{1}{4}F^a_{\alpha\beta}(x)F^a_{\alpha\beta}(x)\right) , \quad \epsilon(x) = -\mathcal{T}_{44}(x)$$

Yanagihara, Iritani, Kitazawa, Asakawa, Hatsuda (2019)

Measuring the flux tube

Connected correlator

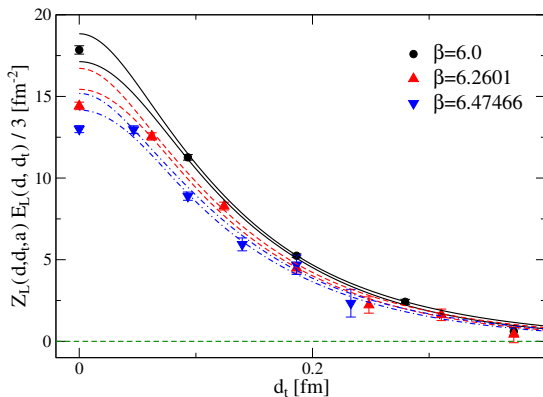$$\rho^{\text{conn}}_{W,\mu\nu} = \frac{\langle \text{Tr}(WLU_PL^*)\rangle}{\langle \text{Tr}(W)\rangle} - \frac{1}{N}\frac{\langle \text{Tr}(U_P)\,\text{Tr}(W)\rangle}{\langle \text{Tr}(W)\rangle} \equiv a^2 g\, F_{\mu\nu}$$

Measuring the flux tube

Connected correlator

$$\rho_{W,\mu\nu}^{\mathrm{conn}} = \frac{\langle \mathrm{Tr}(WLU_PL^*)\rangle}{\langle \mathrm{Tr}(W)\rangle} - \frac{1}{N}\frac{\langle \mathrm{Tr}(U_P)\,\mathrm{Tr}(W)\rangle}{\langle \mathrm{Tr}(W)\rangle} \equiv a^2 g\, F_{\mu\nu}$$

▶ Samples field itself
▶ Gives an average projection onto the color vector defined by the Wilson/Polyakov loop
▶ Ignores fluctuations
▶ Needs renormalization
▶ There is a way to extract the part generating linear behavior

Measuring the flux tube

Connected correlator

$$\rho_{W,\mu\nu}^{\mathrm{conn}} = \frac{\langle \mathrm{Tr}(WLU_PL^*)\rangle}{\langle \mathrm{Tr}(W)\rangle} - \frac{1}{N}\frac{\langle \mathrm{Tr}(U_P)\,\mathrm{Tr}(W)\rangle}{\langle \mathrm{Tr}(W)\rangle} \equiv a^2 g\ F_{\mu\nu}$$

⊘ Batelli, Bonati (2019)

Aims

Zero temperature SU(3)

- ▶ Extract string tension σ from the flux tube,
- ▶ Mean square width w, logarithmic widening,
- ▶ London penetration length λ,
- ▶ Flux tube profile - compare different parametrizations,

Finite temperature SU(3)

- ▶ Disappearance of the flux tube above T_c,
- ▶ Linear widening of the flux tube for T close to T_c,
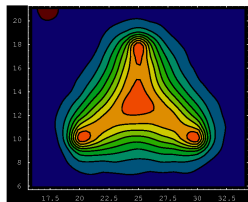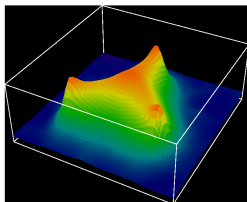
QCD width dynamical fermions

- ▶ Screening and string breaking.

Extensions

Flux tubes for more complex configurations

- ▶ Baryons,
- ▶ Tetraquarks, pentaquarks,
- ▶ "Non-tubes" (diquarks, adjoint quarks).

Extensions

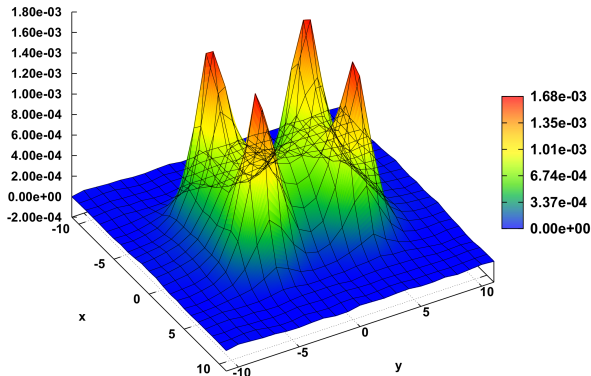Flux tubes for more complex configurations

▶ Baryons,

🔗 Sugunuma, Ichie, Takahashi (2004)

▶ Tetraquarks, pentaquarks,

▶ "Non-tubes" (diquarks, adjoint quarks).

Extensions

Flux tubes for more complex configurations
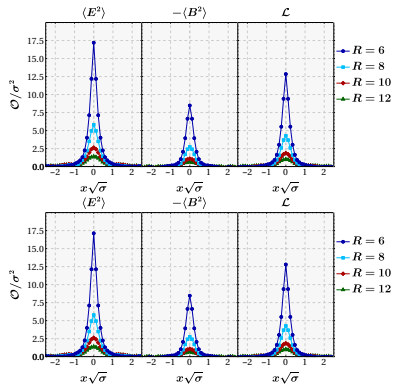
- ▶ Baryons,
- ▶ Tetraquarks, pentaquarks,

Cardoso, Cardoso, Bicudo (2011)

- ▶ "Non-tubes" (diquarks, adjoint quarks).

Extensions

Flux tubes for more complex configurations

- ▶ Baryons,
- ▶ Tetraquarks, pentaquarks,
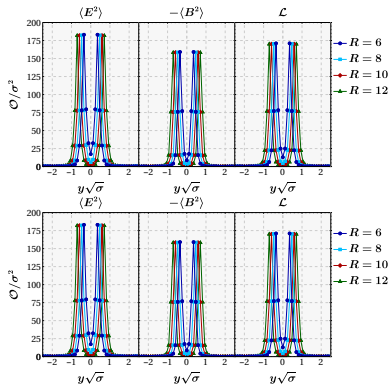- ▶ "Non-tubes" (diquarks, adjoint quarks).

Bicudo, Cardoso, Cardoso (2017)

Extensions

Flux tubes for more complex configurations

- ▶ Baryons,
- ▶ Tetraquarks, pentaquarks,
- ▶ "Non-tubes" (diquarks, adjoint quarks).

🔗 Bicudo, Cardoso, Cardoso (2017)

Subtraction of the "perturbative" field

Full field distribution measured using the connected correlator

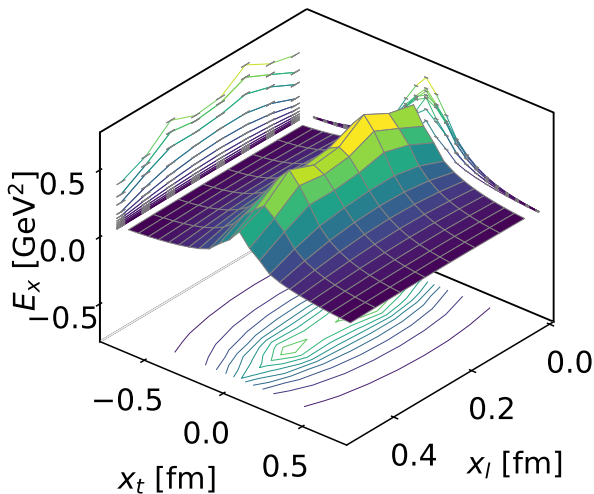To improve the signal-to-noise ratio a smearing procedure was applied:

- one step of 4-dimensional hypercubic smearing on the temporal links (HYPt)
- N_{HYP3d} steps of hypercubic smearing restricted to the three spatial directions (HYP3d)

Results:

- Chromomagnetic field is compatible with zero
- Longitudinal chromoelectric field shows a tube-like structure
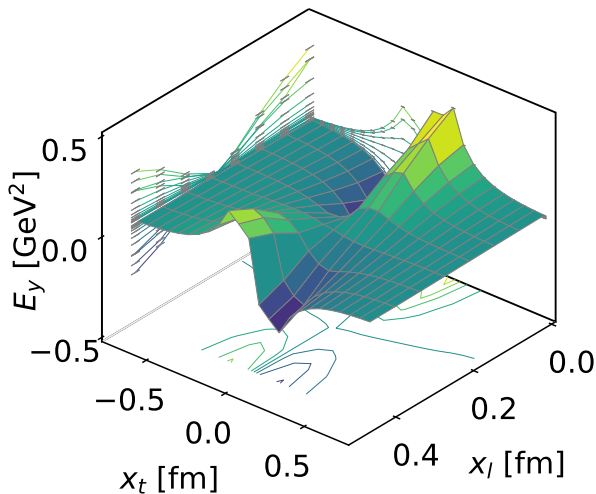- Transverse chromoelectric field is smaller than longitudinal but nonzero

$\beta = 6.240, \, d = 8a = 0.511$ fm

Simulation results: transverse field

$$\beta = 6.240, \ d = 8a = 0.511 \text{ fm}$$

Subtraction procedure

We expect that the full field is a sum of two parts: perturbative part which behaves like an electrostatic field, and nonperturbative part that forms the flux tube
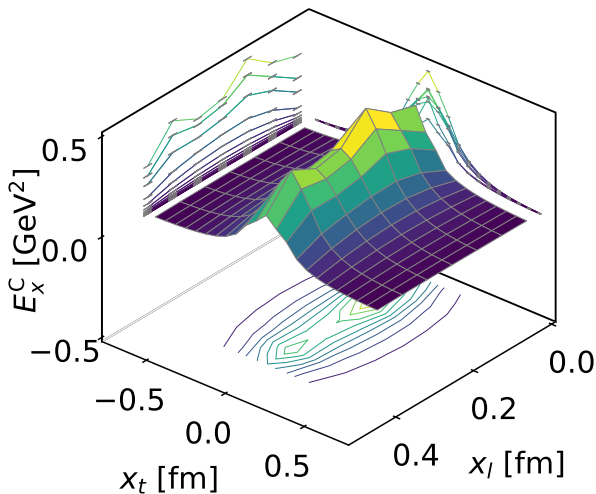
$$\vec{E} = \vec{E}^{\mathrm{C}} + \vec{E}^{\mathrm{NP}}$$

To separate these fields following assumptions are made:

○ $\vec{E}^{\mathrm{C}}$ is a potential field ($\vec{\nabla} \times \vec{E}^{\mathrm{C}} = 0$),

○ $\vec{E}^{\mathrm{NP}}$ is purely longitudinal ($E_y^{\mathrm{NP}} = 0$),

○ both $\vec{E}^{\mathrm{C}}$ and $\vec{E}^{\mathrm{NP}}$ are zero at large transverse separations from the quark-antiquark axis.

These assumptions, together with the calculated values of $\vec{E}$, uniquely determine the field parts.
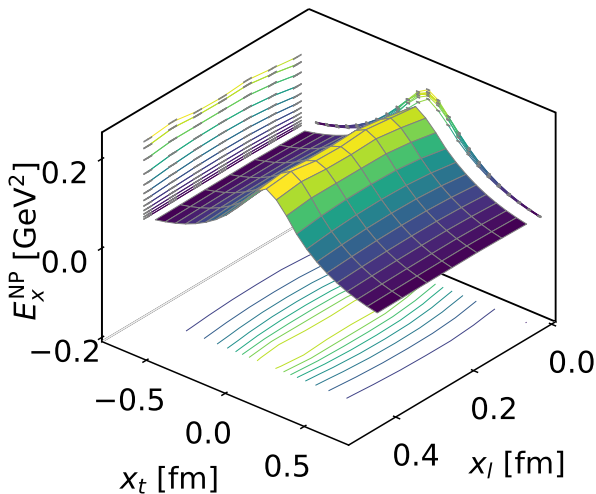
Subtraction procedure: perturbative part

$$\beta = 6.240, \ d = 8a = 0.511 \text{ fm}$$

$\beta = 6.240,\ d = 8a = 0.511$ fm

Field derivatives

Considering that, in our case, the fields are time-independent, and $\vec{B} = 0$, nonzero derivatives of the fields

$$\rho_{\mathrm{el}} = \vec{\nabla} \cdot \vec{E} \ ,$$
$$\vec{J}_{\mathrm{mag}} = \vec{\nabla} \times \vec{E} \ ,$$

allow one to write the force density $\vec{f}$ as

$$\vec{f} = \rho_{\mathrm{el}} \cdot \vec{E} + \vec{J}_{\mathrm{mag}} \times \vec{E} \ .$$

Field derivatives

$$\rho_{\mathrm{el}} = \vec{\nabla} \cdot \vec{E} = \vec{\nabla} \cdot \vec{E}^{\mathrm{C}} + \vec{\nabla} \cdot \vec{E}^{\mathrm{NP}} = \rho_{\mathrm{el}}^{\mathrm{C}} + \rho_{\mathrm{el}}^{\mathrm{NP}}$$

Since the nonperturbative field is purely longitudinal

$$\vec{\nabla} \cdot \vec{E}^{\mathrm{NP}} = \frac{\partial}{\partial x} E_x^{\mathrm{NP}} \ ,$$

We expect the flux tube to be constant in the longitudinal direction, so $\rho_{\mathrm{el}}^{\mathrm{NP}}$ should be close to zero.

$$\vec{J}_{\mathrm{mag}} = \vec{\nabla} \times \vec{E} = \vec{\nabla} \times \vec{E}^{\mathrm{C}} + \vec{\nabla} \times \vec{E}^{\mathrm{NP}} = \vec{J}_{\mathrm{mag}}^{\mathrm{NP}}$$

Due to the rotational symmetry, in our case, the only nonzero component of $\vec{J}_{\mathrm{mag}}$ is $(J_{\mathrm{mag}})_z$ winding around the quark-antiquark axis.

Smearing as an effective renormalization

The connected field operator that we use undergoes a nontrivial renormalization , depending on both x_l and x_t, which has to be taken into account if we want to reach the continuum limit.   ✎ Battelli, Bonati (2019)

Our smearing procedure effectively works as a renormalization, restoring the continuum scaling. To check it we perform simulations on three lattices corresponding to the same physical quark-antiquark distance $d = 0.512$ fm, but having different lattice steps a.
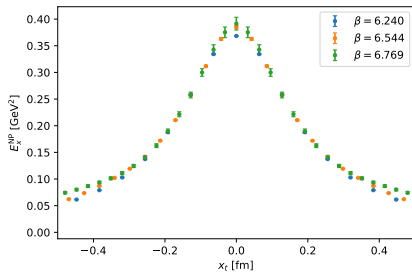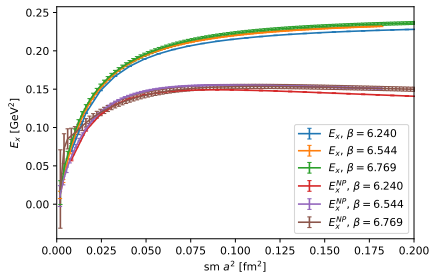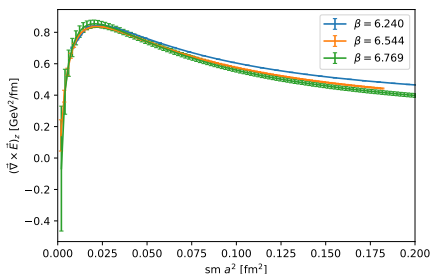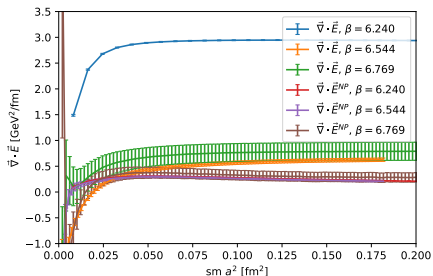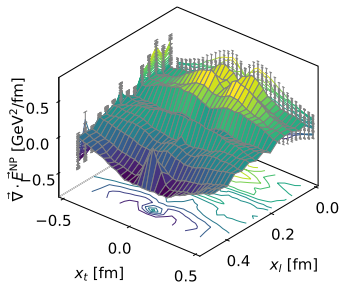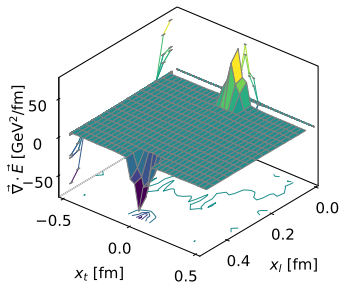
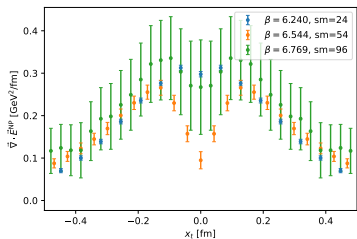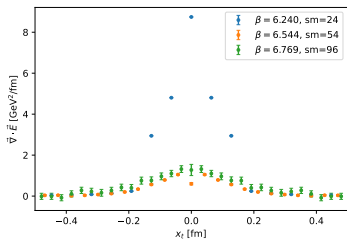# Optimal number of smearing steps

The optimal number of smearing steps depends on

- Observable that we are interested in
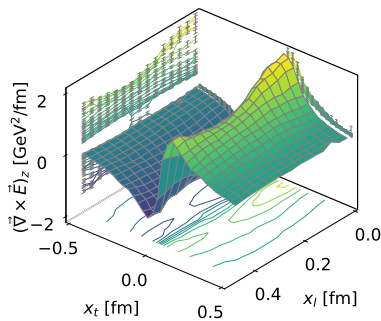- Coordinates x_l and x_t (large coordinates require more smearing steps)

In general, scaling seems to be better at the maximum of the observable.

Electric charge distribution

Magnetic current distribution
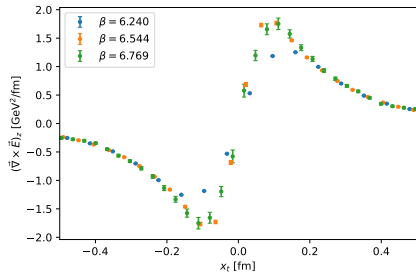
Confining force

Let us cut our space in two by a plane $y = 0$, that contains the quark-antiquark line.

$$\vec{F} = \int_{y>0} d^3\vec{r} \, \vec{J}_{\text{mag}} \times \vec{E}^{\text{NP}} =$$

$$= -2\hat{e}_y \int_0^d \mathrm{d}x_l \int_0^\infty \mathrm{d}x_t \, x_t f^{\text{NP}}(x_l, x_t) \equiv -\hat{e}_y F$$

Force $\vec{F}$ acts perpendicular to the cut plane "squeezing" the flux tube. We estimate this force and compare it with different estimations of the string tension.

String tension

String tension σ can be estimated from the integration of the energy of the nonperturbative field $\vec{E}^{\mathrm{NP}}$ over the transverse cross-section going through the midpoint of the flux tube

$$\sigma_{\mathrm{int}} = \int \mathrm{d}^2 x_t \frac{(E_x^{\mathrm{NP}}(d/2, x_t))^2}{2} =$$
$$= \pi \int \mathrm{d}x_t \, x_t \, (E_x^{\mathrm{NP}}(d/2, x_t))^2 \ .$$

An alternative approach would be to estimate the string tension from the nonperturbative field at the position of the quark

$$\sigma_0 = g E_x(0) \ .$$

Finally, one can compare these results with $\sqrt{\sigma_{\mathrm{NS}}} = 0.464 \ \mathrm{GeV}$ used in setting the physical scale for our simulations $\mathscr{P}$ Necco, Sommer (2002)

Confining force

β	$\sqrt{F}$ [GeV]	$\sqrt{\sigma_{\text{int}}}$ [GeV]	$\sqrt{\sigma_0}$ [GeV]	$\sqrt{\sigma_{\text{NS}}}$ [GeV]
6.240	$0.4859(4)^{+645}$	0.4742(12)	0.56353(81)	
6.544	$0.5165(8)^{+611}_{-214}$	0.4692(16)	0.5962(38)	0.464
6.769	$0.5297(22)^{+547}_{-322}$	0.4672(49)	0.617(16)	

Conclusions

- Field and energy density distributions in the presence of static quark configurations can be measured on the lattice using connected and disconnected correlators, respectively.

- To distinguish confining and nonconfining scenarios on the distances available for simulation, we need a way to separate the field part that generates a linear potential. Such separation is proposed for the field distributions, based on the "zero curl subtraction".

- The string tension σ extracted from the projected field distribution is close to the one obtained from the quark-antiquark potential, suggesting that the average field value along the color direction defined by the source is creating the main contribution to the energy.